# Cumulative fission yield measurements with 14.7 MeV neutrons on $^{238}$U*

**Dr. Arun balaji r, N.Dattathreya, M.MD.IQBAL**
[1]*professor,* [2]*Assistant Professor,*[3] *Associate Professor*
[1,2]*Department of Physics*
*Bheema Institute of Technology and Science, Adoni*

**Abstract:**

Information on the fission yield from the 14 MeV energy neutron-induced fission of 238U is crucial for generation-IV reactor designs and decay heat estimates. Using an off-line γ-ray spectrometric approach, the cumulative yields of fission products ranging from 92Sr to 147Nd in the 238U(n, f) reaction with a 14.7 MeV neutron were measured in order to reliably assess fission product yields (FPYs) of 238U induced by 14 MeV neutrons. The China Academy of Engineering Physics' (CAEP) K-400 D-T neutron generator produced a 14.7 MeV quasi-monoenergetic neutron beam. A low background high purity germanium gamma spectrometer was used to measure fission products. The 93Nb (n, 2n)92mNb reaction yielded the neutron flux, and the cross-section ratios for the 90Zr(n, 2n)89Zr and 93Nb (n, 2n)92mNb reactions were used to compute the mean neutron energy. High precision cumulative yields of 20 fission products were achieved after a series of adjustments. We compared our FPYs for the 238U(n, f) reaction at 14.7 MeV to evaluated nuclear data and the available experimental nuclear reaction data, respectively. The findings will be useful for building evaluated fission yield databases and designing a generation-IV reactor.

**Keywords:** activation process, DT neutron source, fission yields, 238U

## 1. INTRODUCTION

Although nuclear fission was discovered more than 80 years ago, experimental and theoretical studies on it are still far from being complete [1, 2]. Detailed data on the fission cross section, fission-fragment mass, kinetic energy distributions, fission neutron spectrum, and γ-ray spectrum are urgently needed for generation-IV reactor modeling of fuel inventory, reactor decay heat estimation in accident scenario modeling, nuclear material safeguard monitoring, and exploration of nuclear fission theory [3]. Because 238U is associated with 235U in a conventional reactor and with 239Pu in a fast reactor, the fission product yields (FPYs) of 238U at different neutron energies are important for both conventional and fast reactors [4, 5]. With the development of a thorium uranium circulating reactor and a fast neutron breeder reactor, the knowledge of 238U(n, f) fission reaction induced by a 14 MeV neutron is significant. For example, 147Nd plays a key role in nuclear fuel burnup monitoring, and there is a 11.86% discrepancy in previous measured data [3].

Several papers reported that the fission yields for the 14 MeV neutron-induced fission of 238U were measured using radiochemistry and mass spectrometry. The general shape of the mass yield curve has been determined [6–10]. In 1975, D.E. Adams et al. [8] measured 46 mass chain yields of 238U induced by 14.8 MeV neutrons using a radiochemical technique. Although the existing radiochemical technologies could isolate all the fission products, each element presents specific challenges and introduces varying degrees of systematic uncertainties. As one of the most accurate techniques for measuring fission products, mass spectrometry is not suitable for all fission products due to the half-life of fission nuclides.

Numerous investigations on measuring cumulative fission yields by off-line and γ-ray spectrometry are being conducted as a result of the development of the high purity germanium gamma spectrometer

[11– 19]. Recently, a number of studies paid close attention to the dependence of cumulative fission yield on incident-neutron energy. In 2010, J. Laurec et al. [12] performed a series of FPY measurements on 233U, 235U, 238U, and 239Pu in fields of thermal neutrons, fission neutrons, and 14.7MeV neutrons. In 2011, M. Mac Innes [17] determined fission product yields for 14 MeV neutrons on 235U, 238U, 239 and Pu. All studies revealed that the FPY data around 14 MeV neutrons were sparse, owing primarily to the lack of suitable monoenergetic neutron sources.

To address the issue of insufficient precision for FPYs at the 14 MeV neutron energy range, we conduct an investigation with fission induced by 14 MeV neutrons on 238U. Our goal is to perform a thorough high-precision self-consistent study that will provide accurate relative information at the 14 MeV neutron energy range.

## II. EXPERIMENT DETAILS

### A. Target preparation and irradiation

Before using the D-T neutron to induce 238U fission, two natural triuranium octaoxide (U3O8) powder samples (99.9% purity) were made into round disks of 20 mm diameter with thicknesses 1.1 mm (U-1 sample) and 1.0 mm (U-2 sample). Each sample was placed between a Nb foil (diameter: 20 mm, thickness: 0.01 mm, purity: 99.999%) and Zr foil (diameter: 20 mm, thickness: 0.01 mm, purity: 99.99%). A 93Nb(n, 2n)92mNb reaction was used to monitor neutron flux, and the decay data are summarized in Ta- ble 1. Simultaneously, the sandwich sample was covered with a Cd box for preventing scattering of thermal neutrons. During the irradiation, three sandwich samples were placed approximately 6.0 cm away from the T-Ti target relative to the deuteron beam's incident direction at 35° (see Fig. 1).

The irradiation was carried out on the K-400 neutron generator (the yield is approximately $3 \times 10^{10}$ n/4πs) at Institute of Nuclear Physics and Chemistry, China Academy of Engineering Physics. In order to obtain a mass distribution of fission products as completely as possible, the fission product nuclei with different lifetimes should be irradiated in batches. The irradiation time of the U-1 sample was 60 min for the measurement of fission product nuclei with a lifetime of a few hours. To measure longer-lived fission product nuclei, the U-2 sample was irradiated for 17 h. The T(d, n)4He reaction with a deuteron beam (250 keV, 180 μA) produced 14 MeV neutrons. The energies of neutrons were measured using the cross-section ratio of 93Nb(n, 2n)92mNb to 90      89

Zr(n, 2n) Zr reaction and compared with results of mean neutron energy calculation [20, 21], which were 14.7 ± 0.2 at 35°. The Au-Si detector relative to the deu4 teron beam at 135° monitored the accompanying He particle to measure the neutron yield and neutron flux per 10 s, which would give a correction for neutron fluctuation.

### B. HPGe detector efficiency calibration

Before irradiation, a series of standard point sources

**Table 1.** The decay data of monitor reaction and fission products.

| Activation products | Half-life of product $T_{1/2}$ | Gamma-ray energy/keV | Gamma-ray intensity $I^?$ (%) |
|---|---|---|---|
| $^{90}Zr(n,2n)^{89}Zr$ | 78.41±0.12 h | 909.15 | 99.04±0.03 |
| $^{93}Nb(n,2n)^{92m}Nb$ | 10.15±0.02 d | 934.44 | 99.15±0.04 |
| $^{91}Sr$ | 9.65±0.06 h | 1024.3 | 33.5±1.1 |
| $^{92}Sr$ | 2.611±0.017 h | 1383.93 | 90±6 |
| $^{93}Y$ | 10.18±0.08 h | 266.9 | 7.3±1.1 |
| $^{95}Zr$ | 64.032±0.006 d | 756.73 | 54.38±0.22 |
| $^{97}Zr$ | 16.749±0.008 h | 743.36 | 93.09±0.16 |
| $^{99}Mo$ | 65.924±0.006 h | 739.5 | 12.20±0.16 |
| $^{103}Ru$ | 39.247±0.013 d | 610.3 | 5.76±0.06 |
| $^{105}Ru$ | 4.44±0.02 h | 724.4 | 47.3±0.5 |
| $^{127}Sb$ | 3.85±0.05 d | 685.7 | 36.8±2.0 |
| $^{128}Sn$ | 59.07±0.14 min | 482.3 | 59±7 |
| $^{131}I$ | 8.0252±0.0006 d | 364.49 | 81.5±0.8 |
| $^{132}Te$ | 3.204±0.013 d | 228.1 | 88±3 |
| $^{133}I$ | 20.83±0.08 h | 529.87 | 87.0±2.3 |
| $^{134}Te$ | 40.8±0.8 min | 767.2 | 29.5±1.4 |
| $^{135}I$ | 6.58±0.03 h | 1260.41 | 28.7±0.9 |
| $^{140}Ba$ | 12.7527±0.0023 d | 537.26 | 24.39±0.22 |
| $^{142}La$ | 91.1±0.5 min | 641.3 | 47.4±0.5 |
| $^{143}Ce$ | 33.039±0.006 h | 293.27 | 42.8±0.4 |
| $^{147}Nd$ | 10.98±0.01 d | 531.01 | 13.4±0.3 |
| $^{149}Nd$ | 1.728±0.001 h | 270.17 | 10.7±0.5 |
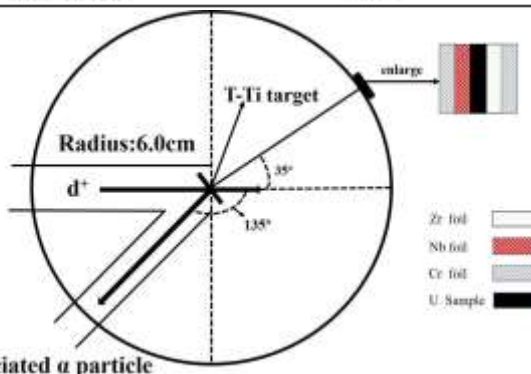


Fig. 1.   (color online) Schematic diagram of experimental geometry [22].

(22Na, 60Co, 133Ba,137Cs, 152Eu) of known activity were used to determine the absolute full energy peak effi- ciency of a lead-shielded high purity germanium detector (HPGe type: GEM60P, produced by ORTEC) with a rel- ative efficiency of 68% and an energy resolution of 1.82 keV at 1.33 MeV for 60Co. The detection efficiencies ($\epsilon_p$ ) for the point source placed at distances of 4.5 cm and 9 cm from the detector were both determined by Eq. (1) [23]:

$$\epsilon_p = \frac{C}{A_0 f e^{-\lambda t}\Delta t I_\gamma},\qquad(1)$$

where C is the number of counts during the counting
time, A0 is the source activity at the time of manufacture, t is the time elapsed from the date of manufacture to the start time of counting, λ is the decay constant, and Iγ is the decay γ intensity.

In order to obtain the detector efficiencies at the char- acteristic γ energies of the fission nuclides, the depend- ence of the full energy peak efficiency versus the energy was described by an exponential function, as expressed in Eq. (2) [24]. The fitting parameter values are given in Fig. 2.

$$\epsilon_p = \frac{C}{A_0 f \cdots^{\lambda t} \Delta t I_\gamma},\qquad (1)$$

C.Measurement of γ-ray activity

After completion of the neutron irradiation and suffi- cient cooling, the two U samples and Nb samples were transferred to a pre-calibrated HPGe detector. The data acquisition was carried out using the program MAES- TRO. By extending the sample cooling time or increas- ing the distance between the sample and the detector, it is possible to significantly lessen the impact of dead time on the statistical count of high purity germanium detectors with high count rate samples. Therefore, the U-1 sample was measured at a distance of 9 cm from the detector
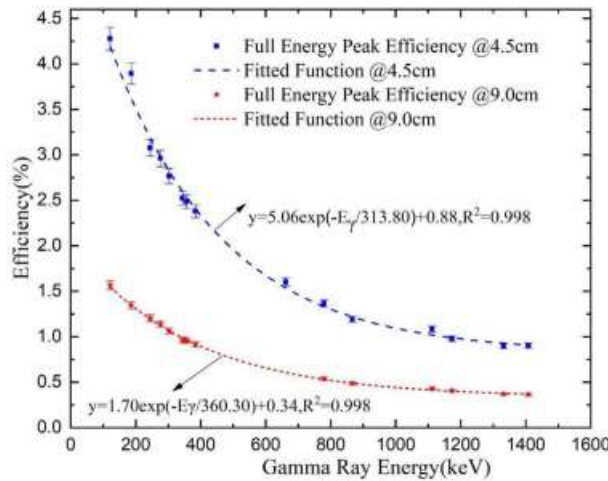


**Fig. 2.** (color online) The fitted efficiency curve and meas-ured efficiency data.

after 76.53 min of cooling. In order to improve the accur- acy of short-lived nuclide counting, it is necessary to per- form dead time correction. The U-1 and U-2 samples were measured after 22.08 h and 20.59 days, respectively, at a distance of 4.5 cm from the detector, and the dead time was negligible.

As shown in Fig. 3, hundreds of different energy characteristic gamma rays were measured by a high-purity germanium detector. In order to identify whether each gamma ray is emitted by the radionuclide of interest, the decay curve analysis method is adopted to identify the radionuclide by measuring the half-life of the radionuclide, which has been discussed in our previous article [25]. We take the 743.36 keV γ-ray produced by the $^{97}$Zr nucleus as an example, which may be affected by the very close energy γ-ray (743.66 keV, 16.1%) from $^{130}$Sn ($T_{1/2}$=3.72
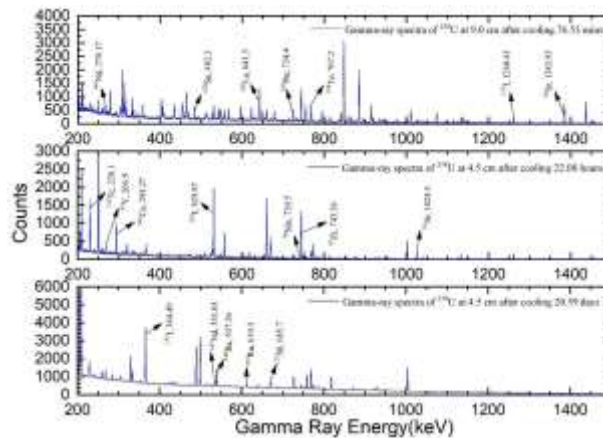


Fig. 3. (color online) The background subtracted gamma spectrum of different fission products of the 238U sample. (a) U-1 sample at 9 cm with 1369 s lifetime; (b) U-1 sample at 4.5 cm with 3600 s lifetime; (c) U-2 sample at 4.5 cm with 10800 s lifetime. min) and by the 743.3 keV (100%) gamma ray from 128Sb (T =9.05 h). Because the half-life of 130Sn is short and the cumulative fission yield of 128Sb is one order of mag- nitude lower than that of 97Zr, there is a good agreement between the half-life obtained by periodical measure- ment as

shown in Fig. 4 (17.04 h) and the recommended half-life (16.75 h) of 97Zr. When the relative deviation between the experimental value and recommended value is less than 5%, it will be selected for the final fission yield calculation [18]. By using this method, twenty char- acteristic gamma rays (as shown in Fig. 4) were selected to calculate the fission yield. The decay characteristics of the product radioisotopes are summarized in Table 1.
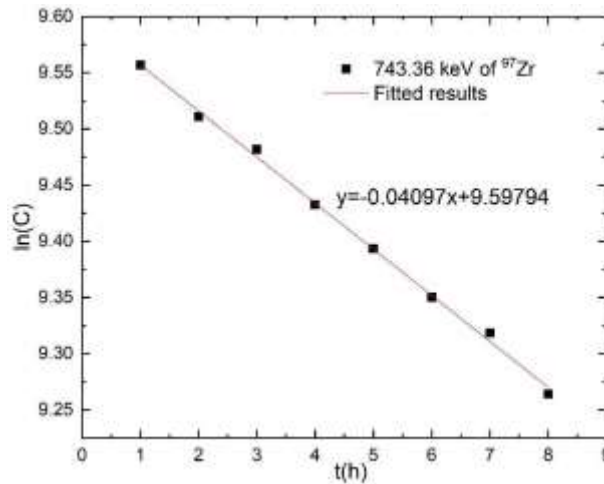


**Fig. 4.**    (color online) Relationship between measurement time of 97Zr and logarithm of characteristic peak counts.

## III. DATA & ANALYSIS

A. Calculation of fission product yields

The number of detected γ-rays corresponding to the activity of fission products was obtained from their total

peak areas by subtracting the linear Compton background. The number of detected γ-rays under the photopeak of an individual fission product is related to their cumulative yields as follows [   4]:

$$Y = \frac{C \lambda f_{all}}{\Phi \sigma_f N_u \epsilon I_\gamma (1 - e^{-\lambda t_1}) e^{-\lambda t_2} (1 - e^{-\lambda t_3})}, \qquad (3)$$

where                                                                          is the net area of the photoelectric peak of the measured characteristic gamma rays; λ is the decay constant of the fission product;
is the fission cross section of 238U at the neutron energy used; is the number of 238U in the target;
is the detection efficiency of the high purity germanium detector system; , , and denote the where C is the net area of the photoelectric peak of the measured characteristic gamma rays; λ is the decay constant of the fission product;σf is the fission cross section of 238U at the neutron energy used;Nu is the number of 238 U in the target;ϵ is the detection efficiency of the high purity germanium detector system;t1,t2, and t3denote the irradiation time, cooling time, and real measurement time, respectively; fall is the correction factor; and Φ is the neutron flux, which can be obtained from the monitor foil Nb as shown in Eq. (4):

$$\Phi = \frac{C' \lambda' f'_{all}}{N' \sigma' \epsilon' I'_\gamma (1 - e^{-\lambda' t_1}) e^{-\lambda' t_2} (1 - e^{-\lambda' t_3})}, \qquad (4)$$

where C′ is the net area of the photoelectric peak of the measured characteristic gamma rays of 92mNb; λ′ is the 92m decay constant of      Nb; σ′ is the cross section of the 93          92m Nb(n, 2n) Nb reaction at the neutron energy used; N′ is the number of 93Nb in the monitor target; ϵ′ is the detection efficiency of the 934.44 keV γ ray in the high purity germanium detector; t1, t2′ , and t3′ denote the irradiation time, cooling time, and real measurement time of the Nb sample, respectively; and fall′ is the correction factor.

### B. Correction factor calculation

In the nuclear reaction data measurement by the activation method there are some corrections such as photon attenuation, neutron flux fluctuation, cascade summing correction, scattered neutron correction, dead time correction, and isotopic impurities. The main correction factor in Eq. (3) and main uncertainty sources are introduced in this section.

1. Photon attenuation Gamma rays are emitted throughout the target volume and experience self-absorption before reaching the detector, which causes the count reduction. Before determining the yield, the self-absorption effect must be corrected to establish the absolute activity of any fission products in the target. According to the attenuation law of γ-rays in matter, the correction factor can be calculated as expressed in Eq. (5):

$$F = \frac{1 - e^{-\mu(E)x}}{\mu(E)x}, \qquad (5)$$

where $\mu(E)$ is the energy-dependent mass attenuation coefficient (cm2·g−1), and x is the product of the material density and "effective" thickness of the sample (g·cm−2). Values for $\mu(E)$ for uranium metal were obtained from the National Institute of Standards & Measurements: XCOM database [26]. According to the ratio of U and O, the total mass attenuation coefficient of different gamma ray energies of U and O materials could be obtained by interpolation.

2. Beam fluctuation correction

The accelerator neutron source cannot be completely stable during long time irradiation; hence, the neutron injection rate fluctuates to a certain extent and needs to be corrected. The correction factor K is calculated using Eq.(6):

$$K = \left[ \sum_{i}^{L} \Phi_i (1 - e^{-\lambda \Delta t_i}) e^{-\lambda T_i} \right] / \Phi S, \qquad (6)$$

where L is number of time intervals into which the irradiation time is divided, $\Delta t_i$ is the duration of the ith time interval, $T_i$ is time interval from the end of the ith interval to the end of irradiation, and $\Phi_i$ is neutron flux averaged over the sample during $\Delta t_i$.

3. Cascade summing correction

For the fission product yield measurement, cascade summing correction is non-negligible. Because of the time consistency, it is possible that one or more of the γrays are simultaneously recorded by the HPGe detector, resulting in the count addition or loss of the characteristic gamma-ray peak. This effect is particularly position dependent for each fission product [18]. The correction factor of cascade summing can be simply written as Eq. (7). A detailed calculation of cascade coincidence correction coefficient can be found in Ref. [27]:

$$C = S/S', \qquad (7)$$

where S is the full-energy peak intensity of the characteristic γ ray if there is no cascade coincidence effect, andS′ is the actual observed full-energy peak intensity of the characteristic γ ray.

The correction factors of photon attenuation, neutron flux fluctuation, and cascade summing correction as well as the total correction factor are summarized in Table 2.

4. Uncertainties

The main uncertainties in the presented measurements are summarized in Table 3, which include photoelectric peak area (0.1%–5%), gamma ray emission probability (0.1% –15%), photoelectric peak detection efficiency (2.0%–3.0%), half-life (0.01%–0.93%), and coincidence summing (3%). The cross-section uncertainty (0.6%) of the 238U(n, f) reaction was obtained by an interpolation method from literature [28]. The total uncertainty (4.62% –16.45%) in the present work is the quadratic summation of the given uncertainties.

## IV. RESULTS AND DISCUSSION

As can be seen from Table 4, twenty cumulative fission product yields were determined for 238U targets at 14.7 MeV incident neutron energy. The given error for each nuclide is the corresponding total uncertainty in the presented experiment. The experimental results in Table 4 were obtained by the direct gamma ray and radiochem

**Table 2.** Values of correction factors.

| Fission products | Photon attenuation | Beam fluctuation | Coincidence summing | Total correction factor |
|---|---|---|---|---|
| $^{91}$Sr | 1.0063 | 0.9991 | 1.0229 | 1.0284 |
| $^{92}$Sr | 1.0049 | 0.9961 | 1.0034 | 1.0044 |
| $^{93}$Y | 1.0586 | 0.9992 | 1.0064 | 1.0645 |
| $^{95}$Zr | 1.0089 | 1.0001 | 0.9848 | 0.9937 |
| $^{97}$Zr | 1.0091 | 0.9996 | 1.0037 | 1.0124 |
| $^{99}$Mo | 1.1401 | 1.0001 | 1.0052 | 1.1461 |
| $^{103}$Ru | 1.0115 | 1.000 | 1.0313 | 1.0432 |
| $^{105}$Ru | 1.0095 | 0.9978 | 1.0124 | 1.0198 |
| $^{127}$Sb | 1.0102 | 0.9950 | 1.0024 | 1.0076 |
| $^{128}$Sn | 1.0165 | 0.9894 | 1.0002 | 1.0059 |
| $^{131}$I | 1.0282 | 0.9961 | 0.9999 | 1.0241 |
| $^{132}$Te | 1.0821 | 1.0001 | 1.0025 | 1.0849 |
| $^{133}$I | 1.0142 | 0.9997 | 1.0815 | 1.0965 |
| $^{134}$Te | 1.0087 | 1.1094 | 1.0012 | 1.1204 |
| $^{135}$I | 1.0052 | 0.9986 | 0.9978 | 1.0016 |
| $^{140}$Ba | 1.0139 | 1.0001 | 1.0145 | 1.0287 |
| $^{142}$La | 1.0109 | 0.993 | 1.0006 | 1.0044 |
| $^{143}$Ce | 1.0430 | 0.9999 | 0.9992 | 1.0421 |
| $^{147}$Nd | 1.0141 | 0.9977 | 1.0075 | 1.0194 |
| $^{149}$Nd | 1.0567 | 0.9939 | 1.0009 | 1.0512 |

**Table 3.** Sources of uncertainties and their magnitudes.

| Source of uncertainty | Magnitude (%) |
|---|---|
| Photoelectric peak area | 0.1–5 |
| Detection efficiency | ≤3 |
| Gamma ray emission probability | 0.1–15 |
| Cross section of $^{238}$U$(n, f)$[26] | 0.6 |
| Half-life | 0.01–0.93 |
| γ-ray absorption | 1 |
| Target mass | 0.01 |
| Neutron flux correction | 0.5 |
| Coincidence summing | ≤3 |
| Total | 4.62–16.45 |

istry method. Adams ' data induced by 14.8 MeV neutrons were measured based on radiochemistry. There exists approximately a 5%–20% difference between presented results and Adams ' data [8]. For the light mass region, the cumulative fission yields in the presented work

are lower than in Adams' work. However, for most nuclides at heavy mass region, the results are higher than Adams ' results, beside 127Sb, 128Sn, and 143Ce. The fission yields of irradiated 238U targets results in M. Innes ' [17] and J. Laurec's [12] works are directly measured by gamma spectrometer without chemical separation. The yields measured in the presented work are comparable with M. Innes' and J. Laurec's works. Comparing with J. Laurec's data, it can be seen that the fission yields obtained by the presented work are consistent with the literature value within the experimental error range, except

for 105Ru,127Sb, and 143Ce. M. Innes 's work is significantly higher than the previous results. Partial discrepancies between the presented work and M. Innes 's data at 14 MeV neutron energy regions are more than 25%. All the results show that the analysis methods of gamma spectrum and data processing in present work are reliable.

As H. Naik showed, the mass chain yields could be obtained from the fission product yields by using a charge distribution correction [4]. However, the difference between the cumulative fission and the mass chain yields is much less than 1%. Thus, the fission product yields are used to substitute the mass chain yields directly. Figure 5(a) shows the presented FPY results and total uncertainties along with the evaluated nuclear data and experimental data in Table 2. Figure 5(b) shows that the majority of discrepancies between evaluations ENDF/B-VIII.0 [29] and JEFF-3.3 [30] are 0.1% –40%. Most of the fission products yields in the presented work are 3% –12% lower than that in ENDF/B-VIII.0 in the light mass region. However, when A=100, the fission yield of JEFF3.3 is 20% higher than that of ENDF/B-VIII.0. Compared with those of ENDF/B-VIII.0, the presented data are in better agreement with JEFF-3.3 in the light mass region. It is obvious that the fission yields of ENDF/BVIII.0 in the heavy mass region have a higher consistency with JEFF-3.3 than those in the light mass region. Except for 127Sb, 128Sn, and 143Ce, the present results are

**Table 4.** Fission product yield results obtained from neutron-induced fission of $^{238}$U around 14 MeV.

| Fission product | Present work at 14.7 MeV | Adams at 14.8 MeV | M. Innes at 14 MeV | J. Laurec at 14.7 MeV |
|---|---|---|---|---|
| $^{91}$Sr | 3.56±0.21 | 4.14±0.37 | 4.89±0.18 | \ |
| $^{92}$Sr | 3.78±0.30 | 3.93±0.42 | \ | \ |
| $^{93}$Y | 3.99±0.63 | 4.63±0.24 | \ | \ |
| $^{95}$Zr | 4.75±0.21 | 5.21±0.27 | 5.48±0.21 | 4.92±0.12 |
| $^{97}$Zr | 5.08±0.22 | 5.55±0.58 | 5.26±0.28 | 5.18±0.14 |
| $^{99}$Mo | 5.40±0.26 | 5.60±0.50 | 5.26±0.20 | 5.79±0.13 |
| $^{103}$Ru | 4.70±0.23 | 5.04±0.28 | 3.40±0.22 | 4.64±0.12 |
| $^{105}$Ru | 2.83±0.13 | 2.90±0.38 | 1.96±0.09 | 3.36±0.15 |
| $^{127}$Sb | 1.05±0.19 | 1.53±0.15 | 2.32±0.16 | 1.35±0.07 |
| $^{128}$Sn | 1.15±0.12 | 1.46±0.19 | \ | \ |
| $^{131}$I | 4.24±0.19 | \ | 4.72±0.21 | 4.08±0.11 |
| $^{132}$Te | 4.91±0.20 | 4.11±0.31 | 4.24±0.17 | 4.72±0.19 |
| $^{133}$I | 5.30±0.24 | 5.68±0.51 | 4.25±0.19 | 5.50±0.24 |
| $^{134}$Te | 6.70±0.34 | 6.35±0.30 | \ | \ |
| $^{135}$I | 5.60±0.30 | 5.39±0.44 | \ | \ |
| $^{140}$Ba | 4.76±0.21 | 4.54±0.40 | 4.67±0.18 | 4.56±0.11 |
| $^{142}$La | 4.08±0.19 | 3.81±0.28 | \ | \ |
| $^{143}$Ce | 2.96±0.13 | 4.25±0.10 | \ | 3.86±0.10 |
| $^{147}$Nd | 2.08±0.11 | 1.97±0.09 | 1.71±0.08 | 1.94±0.10 |
| $^{149}$Nd | 0.97±0.07 | 1.69±0.15 | \ | \ |
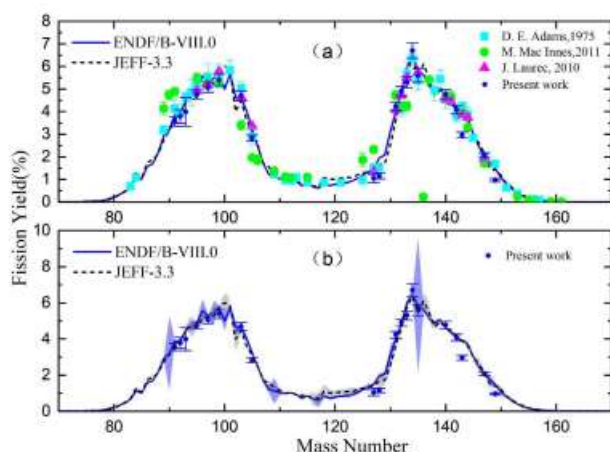


Fig. 5. (color online) Present data compared to the fission product yield distributions from the evaluated nuclear data and experimental data in Table 2 (a). The light blue and light grey areas correspond to the uncertainties of ENDF/B-VIII.0 and JEFF-3.3, respectively (b) consistent with those of ENDF/B-VIII.0 and JEFF-3.3 in the heavy mass region within the uncertainty. There is a lack of evaluation data on the fission yield of 238U with the 14 MeV neutron in the CENDL-3.2 library [31], and the experimental data in this energy region are insufficient; therefore, the present work can lay a foundation for the establishment of the CENDL-3.2 library.

## V. CONCLUSIONS

Using an off-line γ-ray spectrometric approach, a consistent set of high-quality cumulative fission product yield of 238U measurements was measured using 14 MeV neutrons. The quasimonoenergetic neutron

4138

generator was used for the experiment. Following a number of adjustments, the total uncertainty for each of the detected fission products in the 238U(n, f) reaction, ranging from 92Sr to 147Nd, is provided together with the cumulative fission product yields. Overall, the twenty cumulative fission product yields match the available data fairly well. The assessed cumulative fission yield statistics of the 238U reaction at 14 MeV were presented by ENDF/BVIII.0 and JEFF-3.3. Our findings are in line with the JEFF-3.3 assessed yields, however they have a lower light mass peak than ENDF/B-VIII.0. For the majority of mass numbers, the fission yield accuracy was improved. Our methodical measurement establishes the groundwork for the creation of assessed nuclear databases and offers data support for the design of a generation IV reactor.

## References

[1] C. Bhatia et al., Phy. Rev. C 91, 064604 (2015)

[2] X. Sun et al., Chin. Phy. C 39, 014102 (2015)

[3] B. D. Pierson et al., Nucl. Data Sheets 163, 249 (2020)

[4] H. Naika et al., Nucl. Phys. A 941, 16-37 (2015)

[5] Chang-Lin Lan et al., Nucl. Sci. Tech. 28, 8 (2017)

[6] D. J. Gorman et al., Can. J. Chem. 46, 1663-1672 (1968)

[7] L. H. Gevaert et al., Can. J. Chem. 48, 641-651 (1970)

[8] D. E. Adams et al., J. Inorg. Nucl. Chem. 37, 419-424 (1975)

[9] W. X. Li et al., Nucl. Chem. Radiochem. 2, 9 (1983)

[10] C. Chung et al., J. Radioanal. Nucl. Chem. 109, 117-131 (1987)

[11] T. C. Chapman et al., Phys. Rev. C 17, 1089 (1978)

[12] J. Laurec et al., Nucl. Data Sheets 111, 2965-2980 (2010)

[13] H. D. Selby et al., Nucl. Data Sheets 111, 2891-2922 (2010)

[14] E. Dobreva et al., J. Radioanal. Nucl. Chem. 81, 29-36 (1984)

[15] N. Gharibyan et al., J. Radioanal. Nucl. Chem. 303, 1335-1338 (2014)

[16] Q. Sun et al., Nucl. Tech. 40, 070201 (2017)

[17] M. Mac Innes et al., Nucl. Data Sheets 112, 3135 (2011)

[18] M. E. Gooden et al., Nucl. Data Sheets, 131, 319-356 (2016)

[19 Sadhana Mukerji et al., J. Korean Phys. Soc. , 65, 18-24 (2014)

[20] Chang-Lin Lan et al., J. Nucl. Sci. Tech. (2022)

[21] Jun hua Luo et al., Nucl. Instru. Meth. B 298, 61 (2013)

[22] Rong Liu et al., Nuclear Electronics & Detection Technology 19, 428 (1999)

[23] A. Gandhi et al., Phys. Rev. C 102, 014603 (2020)

[24] H. Janssen, Nucl. Instru. Methods A 286, 398 (1990)

[25] Yuting Wei et al., Radiat. Detect. Technol. Methods 6, 361 (2022)

[26] https://physics.nist.gov

[27] X. B. Luo et al., Nucl. Tech. 15, 428 (1992)

[28] A. D. Carlson et al., Nucl. Data Sheets 110, 3215-3324 (2009)

[29] D. A. Brown et al., Nucl. Data Sheets 148, 1-142 (2018)

[30] O. Cabellos et al., EPJ Web Conf. 146, 06004 (2017)

[31] Z. G. Ge et al., EPJ Web Conf. 239, 09001 (2020)